

Supplementary information

Catalytic activity for dissociative oxygen adsorption of Co-based oxides at high temperature evaluated by a modified pulse isotopic exchange technique

Yuto Tomura,^a Toma Tazawa,^a Itaru Oikawa,^a and Hitoshi Takamura^{*a}

^a Department of Materials Science, Graduate School of Engineering, Tohoku University, Sendai 980-8579, Japan.

* Corresponding author email: takamura@material.tohoku.ac.jp

Calibration of the amount of isotope oxygen

In our PIE system, the isotopic gas (He–10% $^{36}\text{O}_2$) for pulses was pre-mixed and stored in a large-volume (> 500 mL) reservoir chamber connecting to a pulse injector and a circulation pump. Because a 4-way valve was used to inject a 1 mL pulse, a small amount (1 mL) of the base gas (N_2 –10% $^{32}\text{O}_2$) is introduced into the reservoir chamber instead of the pulse. It is, therefore, necessary to calibrate the actual amount of isotope oxygen in each pulse injected during PIE measurements. Assuming the same amount of base gas get into the reservoir chamber every time, QMS peak area of $^{36}\text{O}_2$ corresponding the amount of isotope oxygen at n -th pulse, $A(n)$ is expressed by the following formula:

$$A_n = r^{n-1}A_1$$

where r is the dilution rate of isotope oxygen. The actual r value was determined by curve fitting, as shown in Fig. S1. Before starting PIE measurements at high temperature, the amount of isotope in a pulse was measured at room temperature to determine A_1 . The amount of isotope in a pulse injected at each temperature during PIE measurements was calibrated using the formula and the determined r value above. The small temperature dependent changes in f^{in} (indicated by the dashed lines) in Fig. 2 and Fig. S4 are due to this calibration process.

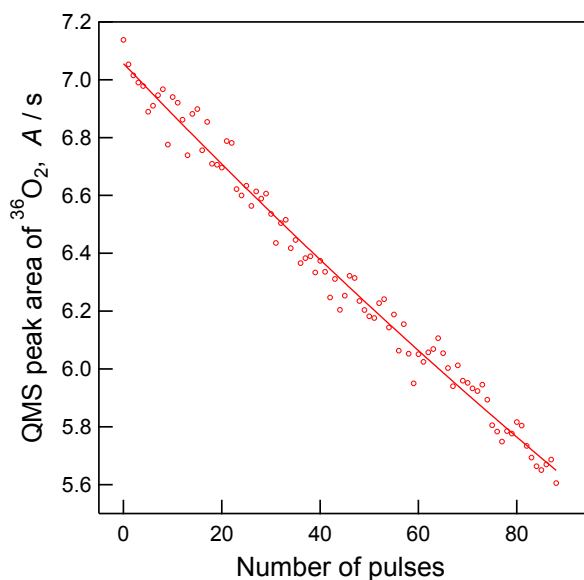


Fig. S1 The QMS peak area of $^{36}\text{O}_2$ in an isotope pulse as a function of the number of injection pulses.

XRD patterns

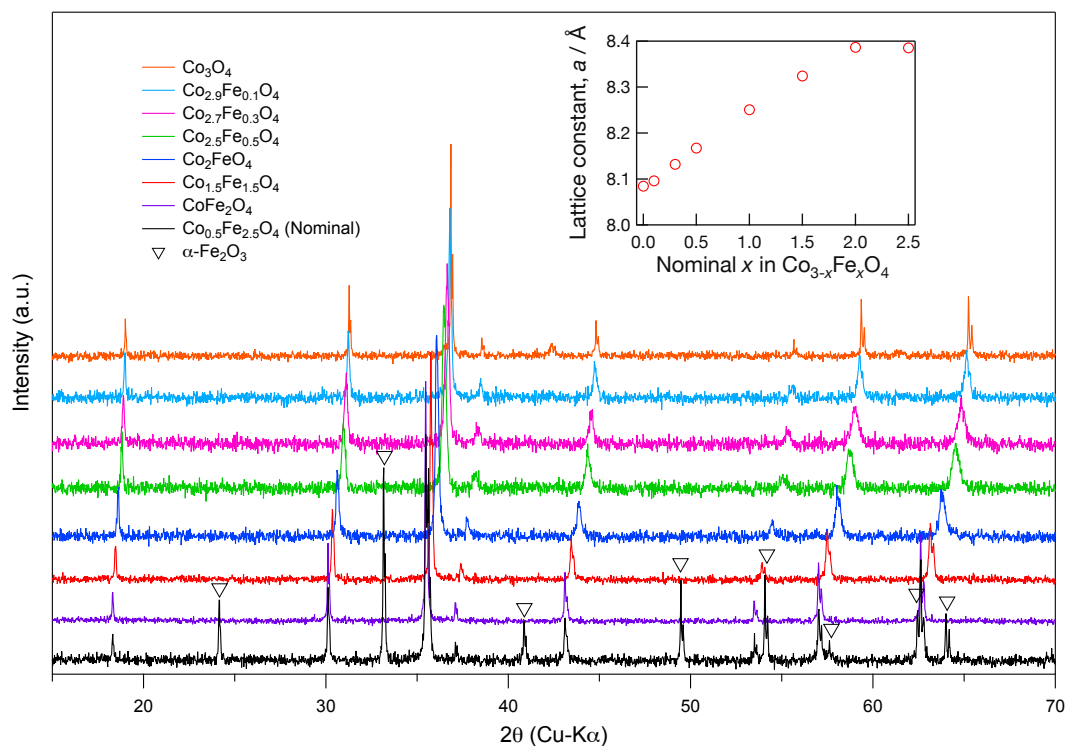


Fig. S2 XRD patterns of Co–Fe-based spinel-type oxides. The lattice constant is plotted as a function of the Fe fraction in the inset.

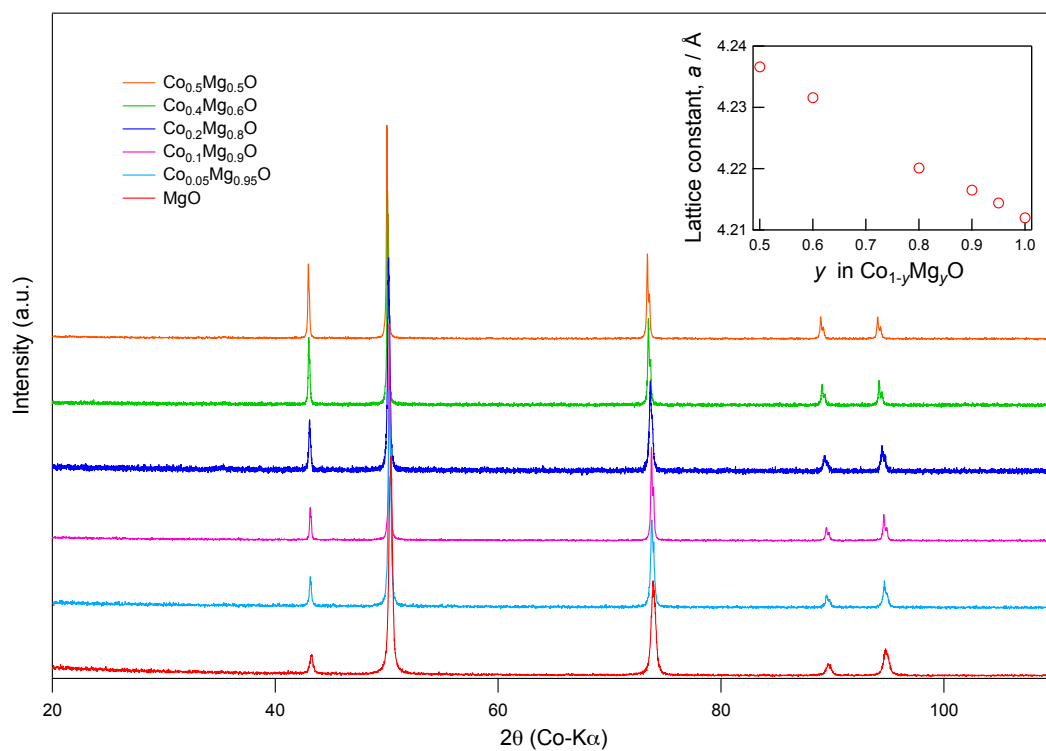


Fig. S3 XRD patterns of Co–Mg-based rock salt-type oxides. The lattice constant is plotted as a function of the Mg fraction in the inset.

ICP-MS

The amount of impurity in some samples was evaluated by ICP-MS (Agilent 8800). 2 mL of hydrochloric acid and 2 mL of nitric acid was added to approximately 10 mg of the powder sample. The sample was then decomposed at 170 °C for five minutes and 210 °C for 55 minutes using a microwave decomposer. This solution was used for ICP-MS analysis. The cation molar fraction of samples and mass concentration of impurities (Al, Si, Y and Zr) are summarized in Tab. S1. The presence of Zr, the major impurity, can be attributed to the planetary ball-mill apparatus made of yttria-stabilized zirconia.

Tab. S1 Composition of the samples analyzed by ICP-MS.

Sample	Cation molar fraction		Impurity/ppm			
	Co	Fe or Mg	Al	Si	Y	Zr
$(\text{Co}_{0.667}\text{Fe}_{0.333})_3\text{O}_4$	0.672	0.326	128	392	73	1168
$(\text{Co}_{0.333}\text{Fe}_{0.667})_3\text{O}_4$	0.343	0.654	231	594	48	637
$\text{Co}_{0.5}\text{Mg}_{0.5}\text{O}$	0.509	0.487	411	686	304	3731
$\text{Co}_{0.2}\text{Mg}_{0.8}\text{O}$	0.203	0.793	200	432	436	5207

Isotope fraction

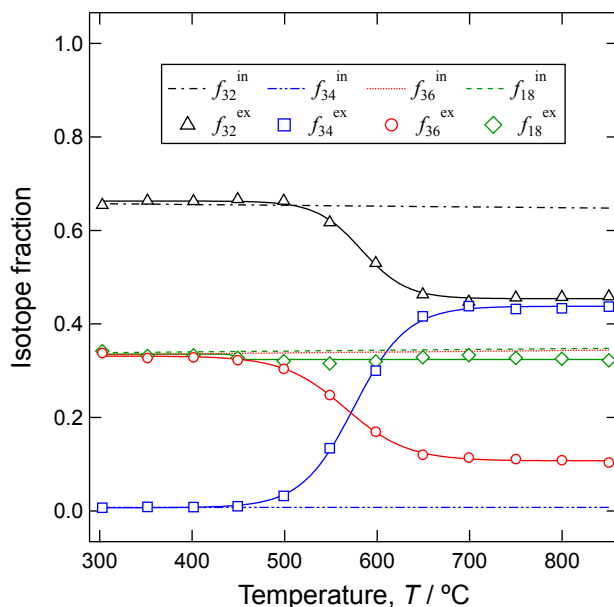


Fig. S4 Isotope fractions of $\text{Co}_{0.4}\text{Mg}_{0.6}\text{O}$ as a function of temperature.

Electrical conductivity

Electrical conductivity was evaluated by four-terminal method and impedance measurements for CoFe_2O_4 and $\text{Co}_{1-y}\text{Mg}_y\text{O}$ ($y = 0.5$ and 0.8), respectively. CoFe_2O_4 and $\text{Co}_{1-y}\text{Mg}_y\text{O}$ were sintered at $1300\text{ }^\circ\text{C}$ for 12 hours and $1400\text{ }^\circ\text{C}$ for 10 hours, respectively. These sintered pellets were polished and then cut into rectangular shapes for CoFe_2O_4 . The Pt paste was baked at $900\text{ }^\circ\text{C}$ on these samples to make electrodes. The temperature dependence of the electrical conductivity evaluated in air is shown in Fig. S5.

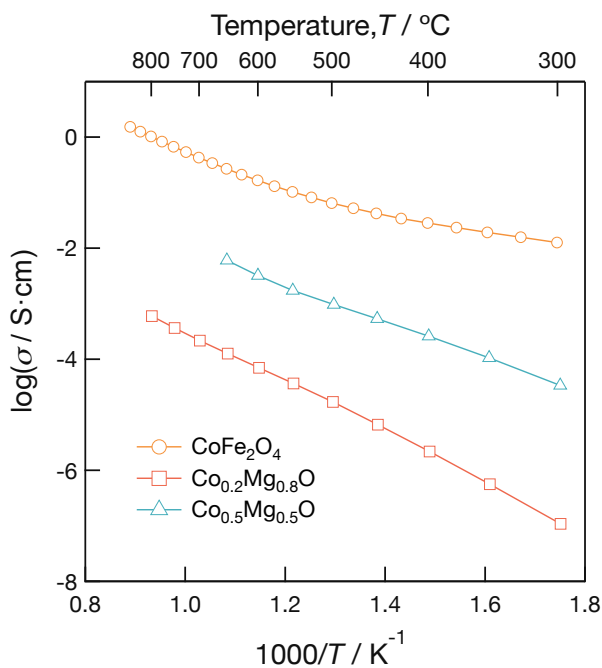


Fig. S5 Arrhenius-type plot of electrical conductivity of CoFe_2O_4 and $\text{Co}_{1-y}\text{Mg}_y\text{O}$ ($y = 0.5$ and 0.8).

Dissociative oxygen adsorption rate

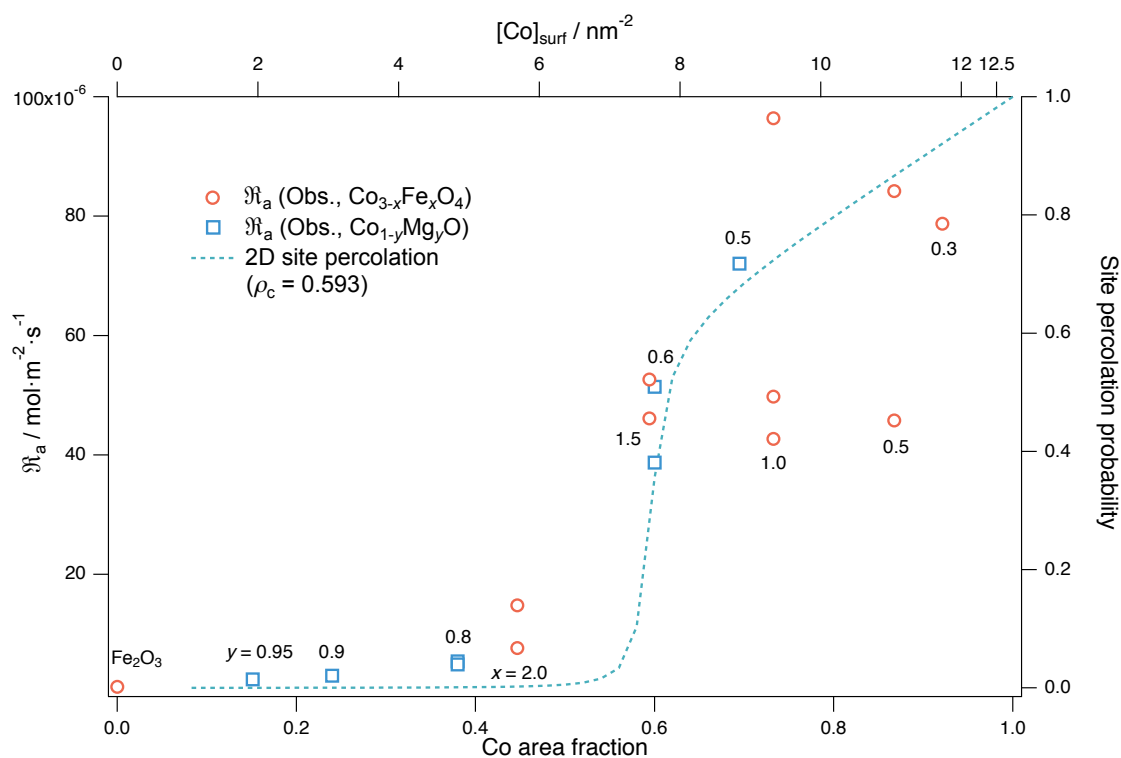


Fig. S6 Dissociative adsorption rates of Co–Fe-based and Co–Mg-based oxides at 600 °C and percolation probability as a function of a normalized nominal Co surface concentration (linear scale).

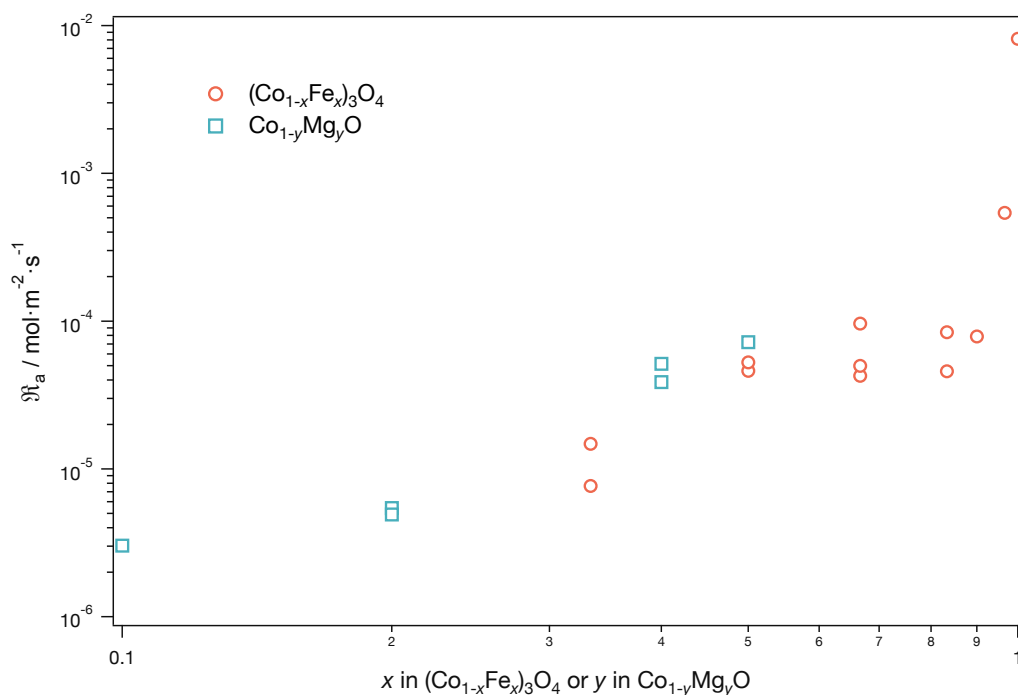


Fig. S7 Dissociative adsorption rates of Co–Fe-based and Co–Mg-based oxides at 600 °C as a function of Fe or Mg fraction.

Activation energy

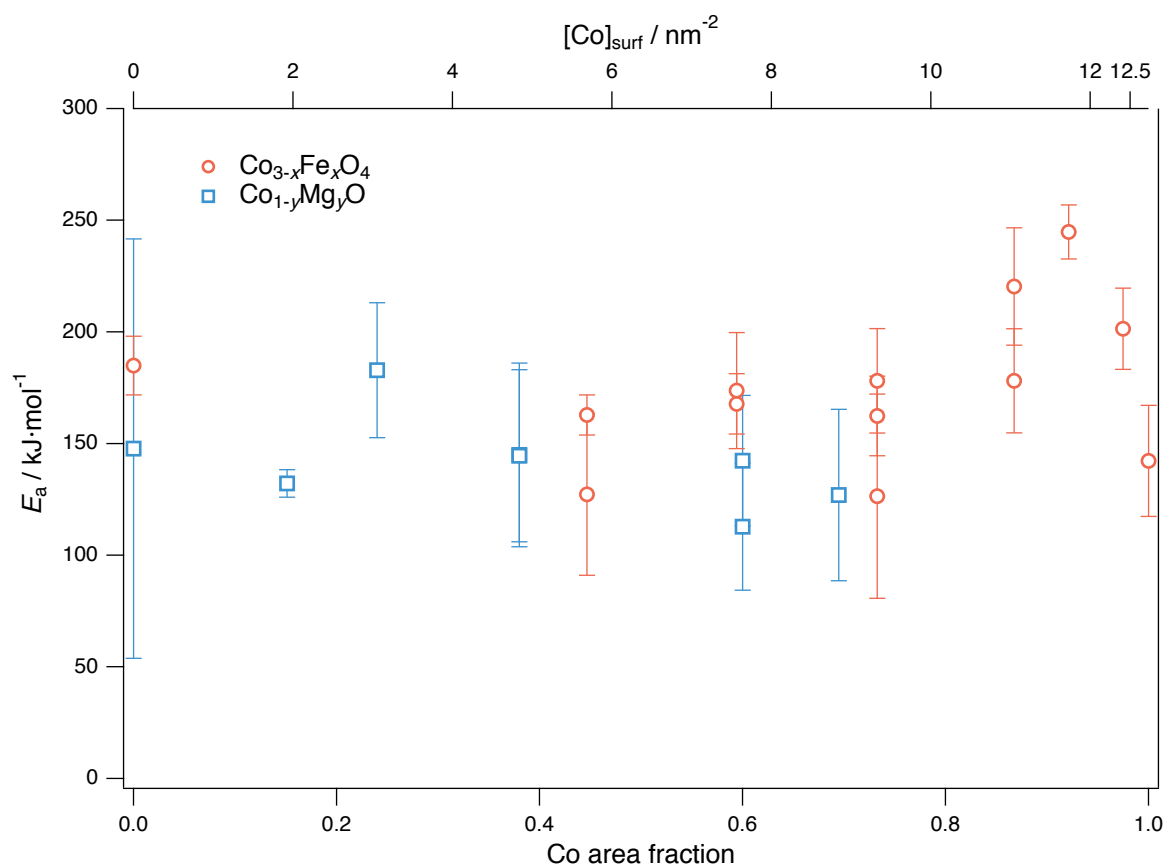


Fig. S8 Activation energy of oxygen dissociation reaction as a function of a normalized nominal Co surface concentration.